J|A|C|S
COMMUNICATIONS

Published on Web 03/21/2006

One-Dimensional Energy/Electron Transfer through a Helical Channel

Oh-Kil Kim,*,† Jongtae Je,† and Joseph S. Melinger‡

Chemistry Division and Electronics Science & Technology Division, and Institute for Nanoscience, Naval Research Laboratory, Washington, D.C. 20375-5320

Received January 6, 2006; E-mail: oh.kim@nrl.navy.mil

A number of molecular devices have been developed for efficient energy/electron transfer (ET/eT) in photo-/electroactive chromophores[1] with a particular interest in artificial photosynthesis. It is well recognized that the electron donor/acceptor (D/A) distance in the chromophores is an important parameter[2] for long-lived charge separation. However, for chain chromophores, the D−A distance parameter alone cannot effectively control the charge recombination due to the conformational flexibility.[3] Part of the solution for this is to rigidify the chromophores by incorporating a stiff linker between D and A subunits.[4] Equally important is achieving efficient transport of electron and energy toward charge separation. This may be facilitated by confinement/shielding of chromophores from unwanted quenching by aggregation and environmental effects.

All these problems can be resolved simultaneously by a supramolecular architecture that is based on a helical encapsulation of chromophores. This device technique is applicable to any chain chromophores as long as they are compatible for encapsulation with a helical polymer of inclusion capability, such as amylose. They do not need any rigid chemical bonds[5] or steric shielding to restrict bond rotation or aggregation, respectively. Earlier, we have developed such a notion and applied it to create amylose-based supramolecules for nonlinear optical and other applications.[6] When confined in the helical cavity, the chromophore is elongated and rigidified along the helical axis. Among advantages gained by encapsulating the chromophores, the most notable one is the large (orders of magnitude) enhancement of the fluorescence quantum yield, which results from single molecular confinement in the rigid and quenching-free environment,[6a−c] and also remarkable photo/thermal stabilities.[7] A distinct feature of the supramolecular system is the formation of oriented self-assembled thin films[6b,8] upon casting aqueous solution since either amylose or chromophore alone is unable to do it.

In this communication, we report highly efficient one-dimensional ET/eT of amylose-encapsulated chromophores, which are designed bidirectionally from the central D to the terminal A units along the helical channel. We observed that the eT of the encapsulated chromophores exhibits a clear dependence on the D−A distance and the A strength, contrasting strongly to that of the encapsulation-free counterparts.

We have synthesized (S-1) a series of A−D−A chromophores, where D is oligo(phenylene vinylene), OPV (D), and A is pyridinium, *N*,*N*′-dialkyl-4,4′-bipyridinium and *N*,*N*-dimethylaminostyryl-4-pyridinium (DASP) moieties, and the D/A subunits are linked by an alkyl chain spacer. Electron/energy transfers of the chromophores were investigated in aqueous solution with amylose encapsulation and free of encapsulation for reference. These A−D−A chromophores are all remarkably adaptable to the helical inclusion by amylose. We have observed strong evidence for the helical inclusion of the chromophores, which is represented by OPV−II−12 (S-2), featuring that a steady decrease of the absorption at around $\lambda_{max} = 330$ nm occurs upon the addition of amylose, accompanied by a concomitant increase in a new red-shifted absorption at $\lambda_{max} = 375$ nm. This indicates a molecular transition from the aggregation state to the single molecular encapsulation by amylose. Exactly the same pattern of increase is observed in the fluorescence intensity ($\lambda_{em} = 432$ nm) with increasing amylose, accounting for $>10^3$ enhancement. Further evidence for helical inclusion is the observation of a distinctive circular dichroism of the OPV (S-2) induced by the host helix and fluorescence excitation profile/fluorescence spectra (S-2) that are invariant to excitation/collection wavelengths.

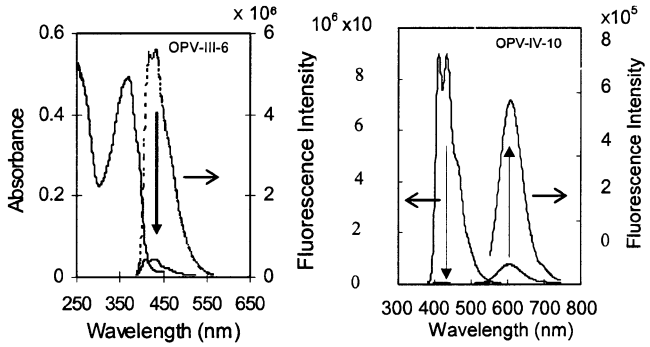

Figure 1. Electron and energy transfer in helically encapsulated OPV-based chromophores by excitation of the OPV unit (D) at 375 nm: (*left*) decrease in fluorescence intensity of the OPV unit in OPV−III−6 due to eT to viologen moiety (A) from the OPV unit (represented by OPV−II−12) in water; [OPV−III−6]/[amylose] = 1×10^{-5} M/1×10^{-3} M for ABS, and 1×10^{-6} M/1×10^{-4} M for FL spectra; and (*right*) fluorescence quenching of OPV and concomitant enhanced fluorescence intensity of the DASP unit (A) in OPV−IV−10 due to ET from the OPV unit (D) in 25% DMSO; [OPV−IV−10] = 1×10^{-5} M, [amylose] = 1×10^{-3} M.

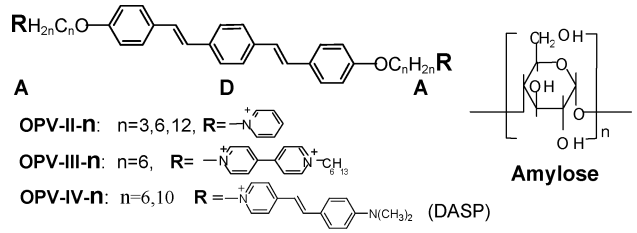

Figure 1 (*left*) shows photoinduced eT of OPV−III−6, confined in an amylose helix, which was determined based on the fluorescence quenching of the OPV unit (D) by the viologen residue (A), where the blue emission of OPV at 432 nm is almost completely quenched (>95%). The initial fluorescence intensity of the OPV unit (without A) is represented by OPV−II−12 ($\lambda_{em} = 432$ nm) because its emission is unaffected by the presence of a weak A (pyridinium) with the long alkyl spacer (C_{12}) and, thus, extrapolated as a control in the Figure. Figure 1 (*right*) shows through-space

† Chemistry Division.
‡ Electronics Science & Technology Division.

10.1021/ja060122c CCC: $33.50

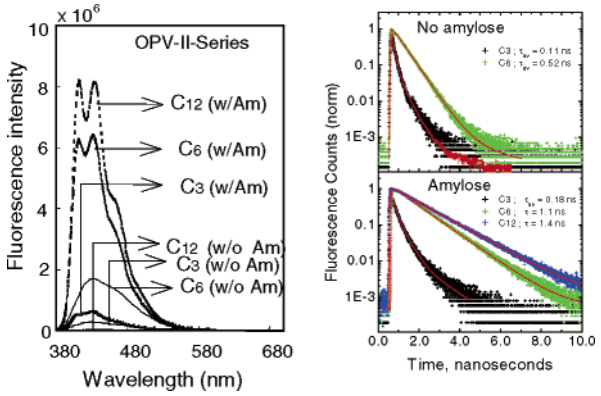

Figure 2. Dependence of fluorescence intensity (*left*) and fluorescence decay rate (*right*) of OPV−II chromophores (with and without amylose) on D−A distance (Cn); [OPV−II−series] = 1×10^{-5} M, [amylose] = 2×10^{-3} M in water (1% DMSO).

ET between OPV and DASP (A) units in OPV−IV−10 with the helical encapsulation. For this molecule, the emission band of OPV and the absorption band of DASP are well overlapped (S-3). In this case, as in the case of OPV−III−6, OPV−II−12 fluorescence is used as the initial (without A) OPV fluorescence. For OPV−IV−10, the initial OPV fluorescence is nearly completely quenched (>99%)[9a] by the DASP unit (A) upon excitation of the OPV unit, and the subsequent ET excitation of the DASP unit brings about a large enhancement (>10-fold)[9b] in DASP fluorescence ($\lambda_{em} = 620$ nm). A Förster-type calculation using a dyad model of OPV−IV−10 confirms the efficient ET observed experimentally (S-4).

On the other hand, the free OPV−III−6 (without amylose) shows a much larger decrease (S-5) in the OPV fluorescence intensity (at 432 nm), compared to that of the encapsulated counterpart (vide supra). Similarly, but for different reasons, the encapsulation-free OPV−IV−10 also exhibits an extremely low OPV emission intensity (at 432 nm) relative to the encapsulated counterpart.[10] The former (OPV−III−6) may be due to conformational flexibility in water, which promotes collisional quenching, and the latter (OPV−IV−10) is due to a dominant aggregation, such that there is no measurable differences in the intensity by exciting either OPV (at 370 nm) or DASP itself (at 480 nm). These clearly suggest that the unusually low fluorescence intensities (of OPV) for the free OPV−III−6 and the free OPV−IV−10 are not the result of a complete eT/ET.[11] In this regard, it is particularly significant for the encapsulated counterpart to observe a well-defined photoinduced eT with a remarkable efficiency over the distance of 10 Å or more.

Compared to OPV−III−6, the extent of eT in OPV−II−6, for example, is much smaller due to the weak A strength. Nonetheless, the weakness of the A strength can make the degree of eT more distinguishable by D−A distance. Particularly, the facile encapsulation with helical amylose makes the OPV−II series of chromophores more attractive for studying the distant dependence. As shown in Figure 2 (*left*), the eT of OPV−II chromophores, when encapsulated, exhibits a strong dependence on the spacer length, indicating that the chromophore with a C_3 spacer has the largest eT (decrease in the fluorescence intensity) and the one with C_{12} has a negligible eT.

On the basis of the fluorescence quenching and lifetime data (Figure 2, *right*), eT rates of encapsulated C_3 and C_6 chromophores are estimated to be 6.8×10^9 and 0.21×10^9 s^{-1}, respectively (S-4). It was further confirmed that the eT in the encapsulated chromophores depends explicitly on the A strength (S-6): ammonium < pyridinium < viologen. In contrast, the eT quenching for the encapsulation-free counterparts has mixed contributions from both the distance effect and nonradiative deactivation by aggregation and/or collisional quenching.[3] These are closely related to the environmental sensitivity (S-7) of the free chromophores and are reflected in their low fluorescence quantum yields[12] and very short lifetimes, particularly for the encapsulation-free OPV−II−12 due to a strong aggregation (S-7). On the contrary, the electronic coupling of the D−A chromophores confined in the amylose helix is little affected by local environment (S-7), so that one-dimensional event of transport prevails.

In conclusion, we have synthesized A−D−A chain chromophores based on OPV as an electron donor (D) and several electron/energy acceptors (A), which are linked by various alkyl spacers. Photoinduced electron/energy transfers (eT/ET) of the chromophores are investigated in the presence and absence of helical encapsulation with respect to D−A distance and A strength. The fluorescence intensity (of OPV unit) of the encapsulation-free chromophores is unexpectedly small, not due to the advancement of eT but more likely to self-quenching by aggregation and/or conformational flexibility. By contrast, the helically encapsulated counterparts exhibit a remarkable photoinduced eT/ET with a well-defined distance and A strength effects. The work related to this is in progress.

Acknowledgment. The authors acknowledge partial funding support from the Office of Naval Research and the Defense Advanced Research Projects Agency.

Supporting Information Available: Material synthesis and spectroscopic details are given. This material is available free of charge via the Internet at http://pubs.acs.org.

References

(1) (a) Balzani, V.; Venturi, M.; Credi, A. *Molecular Devices and Machines*; Wiley-VCH: Weinheim, Germany, 2003; pp 33−176. (b) Gust, D.; Moore, T. A.; Moore, A. L. *Acc. Chem. Res.* **2001**, *34*, 40−48.

(2) (a) Fox, M. A. *Acc. Chem. Res.* **1992**, *25*, 569−574. (b) Wasielewski, M. R. *Chem. Rev.* **1992**, *92*, 435−461. (c) Luo, C.; Guldi, D. M.; Imahori, H.; Tamaki, K.; Sakata, Y. *J. Am. Chem. Soc.* **2000**, *122*, 6535−6551.

(3) Lakowicz, J. R. *Principles of Fluorescence Spectroscopy*, 2nd ed.; Kluwer Academic/Plenum Publishers: New York, 1999; Chapters 8 and 14.

(4) (a) Bell, T. D. M.; Smith, T. A.; Ghiggino, K. P.; Ranasinghe, M. G.; Shephard, M. J.; Paddon-Row, M. N. *Chem. Phys. Lett.* **1997**, *268*, 223−228. (b) Liddle, P. A.; Kuciauskas, D.; Sumida, J. P.; Nash, B.; Nguyen, D.; Moore, A. L.; Moore, T. A.; Gust, D. *J. Am. Chem. Soc.* **1997**, *119*, 1400−1405.

(5) (a) Davis, W. B.; Ratner, M. A.; Wasielewski, M. R. *J. Am. Chem. Soc.* **2001**, *123*, 7877−7886. (b) Kilsa, K.; Kajanus, J.; Macpherson, A. N.; Martensson, J.; Albinsson, B. *J. Am. Chem. Soc.* **2001**, *123*, 3069−3080.

(6) (a) Kim, O.-K.; Choi, L.-S. *Langmuir* **1994**, *10*, 2842−2846. (b) Kim, O.-K.; Choi, L.-S.; Zhang, H.-Y.; He, X.-H.; Shih, Y.-H. *J. Am. Chem. Soc.* **1996**, *118*, 12220−12221. (c) Kim, O.-K.; Choi, L.-S.; Mlsna, T. E.; McGill, R. A.; Zhang, H.-Y.; He, X.-H.; Shih, Y.-H. *Nonlinear Optics* **1999**, *20*, 157−168. (d) Kim, O.-K.; Je, J.; Baldwin, J. W.; Kooi, S.; Pehrsson, P. E.; Buckley, L. J. *J. Am. Chem. Soc.* **2003**, *125*, 4426−4427. (e) Kim, O.-K.; Je, J.; Jernigan, G.; Buckley, L.; Whitten, D. *J. Am. Chem. Soc.* **2006**, *128*, 510−516.

(7) (a) Lau, S.-F.; Sosnowik, A. J.; Choi, L.-S.; Callahan, J. H.; Kim, O.-K. *J. Therm. Anal.* **1996**, *46*, 1081−1092. (b) Choi, L.-S.; Kim. O.-K. *Macromolecules* **1998**, *31*, 9406−9408.

(8) Kim, O.-K.; Jernigan, G.; Pepitone, M.; Melinger, J. S. Unpublished results.

(9) (a) The initial intensity of OPV fluorescence decreased from 8×10^6 to 5×10^4. (b) Fluorescence intensity of encapsulated DASP was measured by selective excitation at 480 nm (w/o ET) to be $\sim 5 \times 10^4$, while the ET-induced fluorescence intensity of DASP was $> 5 \times 10^5$ in 25% DMSO.

(10) For the free OPV−IV−10 (without amylose), the fluorescence intensity of OPV ($\lambda_{em} = 432$ nm) is negligibly small, 1×10^3 (in 25% DMSO), while for the encapsulated counterpart, that is 4×10^4 under the same scale.

(11) Extremely small OPV fluorescence intensities from the encapsulation-free OPV−III−6 and OPV−IV−10 are not the consequence of eT and ET, respectively, but are due to aggregation quenching (see S-5 and S-7 in the Supporting Information).

(12) Fluorescence quantum yields of OPV−II−3, −6, and −12 are measured using quinine sulfate as the standard, 0.03, 0.40, and 0.65, respectively, for the encapsulated chromophores, and 0.02, 0.19, and <0.01, respectively, for encapsulation-free counterparts.

JA060122C